photonics

MDPI

Article

Temperature Control Performance Improvement of High-Power Laser Diode with Assistance of Machine Learning

Yaohui He [1,2], Xiaoli Jin [1,3], Pixian Jin [1,3], Jing Su [1,3], Fang Li [4,*] and Huadong Lu [1,3,5,*]

1 State Key Laboratory of Quantum Optics Technologies and Devices, Institute of Opto-Electronics, Shanxi University, Taiyuan 030006, China; heyh@sxu.edu.cn (Y.H.); jinxiaoli@sxu.edu.cn (X.J.); pxjin@sxu.edu.cn (P.J.); jingsu@sxu.edu.cn (J.S.)
2 College of Physics and Electronic Engineering, Shanxi University, Taiyuan 030006, China
3 Collaborative Innovation Center of Extreme Optics, Shanxi University, Taiyuan 030006, China
4 Shanxi Bethune Hospital, Shanxi Academy of Medical Sciences, Third Hospital of Shanxi Medical University, Tongji Shanxi Hospital, Taiyuan 030032, China
5 National Key Laboratory of Particle Transport and Separation Technology, Tianjin 300181, China
* Correspondence: lifang@sxmu.edu.cn (F.L.); luhuadong@sxu.edu.cn (H.L.)

Abstract: For a laser diode (LD) with high output power, it is difficult to precisely and quickly control its temperature because of the large thermal power involved. In this paper, a machine learning-based temperature controller for high-power LDs is reported. It is implemented by developing a back-propagation neural network (BPNN) with an adaptive dynamic adjustment strategy (ADAS) temperature controller which integrates a constant-current-source circuit into the conventional proportional-integral-derivative (PID) temperature-controlling circuit. Compared to the conventional PID controller, the speed of temperature control had been shortened from 1300 s to 350 s, the long-term temperature fluctuation was decreased from ±0.148% to ±0.082%, and the step response time could be decreased from 960 s to 210 s.

Keywords: laser diode (LD); all-solid-state lasers; temperature control; machine learning; BP neural network (BPNN)

check for updates

Received: 2 February 2025
Revised: 28 February 2025
Accepted: 5 March 2025
Published: 7 March 2025

Citation: He, Y.; Jin, X.; Jin, P.; Su, J.; Li, F.; Lu, H. Temperature Control Performance Improvement of High-Power Laser Diode with Assistance of Machine Learning. *Photonics* **2025**, *12*, 241. https://doi.org/10.3390/photonics12030241

Copyright: © 2025 by the authors. Licensee MDPI, Basel, Switzerland. This article is an open access article distributed under the terms and conditions of the Creative Commons Attribution (CC BY) license (https://creativecommons.org/licenses/by/4.0/).

1. Introduction

It is well known that laser diodes (LDs) are important pump sources of solid-state and fiber lasers [1]. In order to achieve a stable laser with high optical efficiency, it is necessary to precisely control the temperature of the LD because temperature fluctuation can cause wavelength drift and power fluctuation [2,3]. In order to address this issue, a thermoelectric cooler (TEC) [4,5] based on the Peltier effect [6–8] and a copper board are often employed as the heat transfer element and heat sink [9], respectively. At the same time, a proportional-integral-derivative (PID) control system is adopted to achieve the auto-temperature control [10]. In recent years, in order to increase the temperature-controlling speed, tuning and optimizing PID algorithms using mathematical methods to address dead-time processes have been developed, which could enable the automatic tuning of PID controllers, such as self-tuning [11,12] and auto-tuning [13] controllers. In 2011, Xing et al. [14] introduced a Ziegler–Nichols tuning method into an LD temperature control system to model temperature characteristics, improving the accuracy of the control system. However, mathematical methods in PID controllers require the establishment of precise mathematical models based on specific principles, making it challenging to handle the nonlinearity, uncertainty, and time-varying characteristics of complex environments. To overcome this problem, in 2010, Cong et al. [15] developed a digital LD temperature control

system centered on a digital signal processor (DSP) and utilized the Fuzzy-PID algorithm to regulate the output power of a thermoelectric cooler (TEC). The control system achieved a stability of approximately ±0.1 °C over 2 min and could optimize PID parameters in real time. In 2023, Jian et al. [16] adopted an advanced PID controller optimized by particle swarm optimization (PSO-PID) to resolve real-time PID parameters for different inputs using a field programmable gate array (FPGA) in an LD temperature control system. And a temperature stability of 0.2% over 2 h was attained, which effectively reduced the power instability and wavelength deviation. Although these intelligent control methods [17–20] can enhance the step response of nonlinear and real-time systems and further offer great efficiency in terms of hardware resource utilization, they were demonstrated in LDs with low power. Moreover, it can be seen that the parameters of conventional PID algorithms are typically determined through extensive testing and cannot be optimized in real time with the environmental condition variation [21,22]. Later, the machine learning [23] based on BPNN [24–26] was gradually developed and applied in auto-controlling fields owing to its intrinsic advantage of complex data processing, good adaptability to ambient environmental variations, strong predictability, and optimization capabilities [27–30].

In order to enhance the precision and speed of temperature control for an LD with high output power, in this paper, we first integrated a constant-current-source circuit into a conventional PID temperature-controlling circuit. Then, a BPNN with an adaptive dynamic adjustment strategy (ADAS) was developed to actively optimize and adjust the temperature control unit by performing real-time analysis of temperature differentials, thereby enhancing its capability to efficiently manage significant temperature fluctuations caused by high heat and achieving rapid and stable temperature regulation. Lastly, when the conventional PID and BPNN-PID temperature controllers were replaced by the BPNN with an ADAS temperature controller, the temperature controlling speed was shortened from 1300 s and 875 s to 350 s, while the precision decreased ±0.148% and ±0.146% to ±0.082%, and the step response time decreased from 960 s and 540 s to 210 s.

2. Experiment Design

In the experiment, an intelligent control system (ICS) was employed as a terminal controller to monitor and control the real-time temperature of the LD through an LD temperature control device (LD-TCD). The designed intelligent LD temperature controller was shown in Figure 1a. To mitigate the effects of the ambient airflow and temperature drift [31,32] of the LD, the LD was placed in a relatively confined space. The structural details of the designed LD temperature control device (LD-TCD) are illustrated in Figure 1b. A heat plate was utilized to mount the LD to facilitate efficient heat transfer. The lower surface was closely attached to four thermoelectric coolers (TECs) with sizes of 40 mm ∗ 40 mm ∗ 3.45 mm for effective heat conduction between the heat plate and the heat sink. To achieve heat dissipation as soon as possible, the heat sink was equipped with microchannel water cooling and connected to a water circulation system. To prevent the devices from being damaged, the water flow rate was set to 6.2 L/min.

When the employed LD operated at a temperature of 25 °C, the emission wavelength [33] was centered at 888 nm [34]. The output power reached up to 110 W with a supply current and a voltage of 51 A and 3.95 V, respectively. In this case, the electrical-to-optical conversion efficiency was merely 54.6%, which meant that a thermal power of up to 91.5 W was generated. It was basically impossible to achieve fast temperature control for such a large thermal power by using the conventional PID controlling [35]. In order to overcome this problem, a constant-current-source circuit, depicted in Figure 2, was integrated into the conventional PID temperature-controlling circuit. And the whole framework of the control system is illustrated in Figure 3, which was implemented by utilizing a

microcontroller unit (MCU) based on a digital signal processor (DSP) chip (TMS320F28069) for data processing and instruction execution. When the current of the drive source of the LD was continuously increased, the thermal power proportionally increased with the increase in the LD driving current. At this time, the constant-current-source circuit would provide a corresponding current to the TEC4 through its negative feedback loop according to the drive current of the LD to quickly control the temperature of the LD near the set value. Meanwhile, the system continuously acquired real-time temperature data T_m using a thermistor TCS610 (NTC, 10 kΩ, 25 °C) and transmitted the data to the MCU. The MCU calculated the real-time temperature difference and generated a high-resolution pulse-width modulation (HRPWM) signal through the PID algorithm, which was transmitted to the DRV8432 to supply drive current to a set of parallel thermoelectric coolers (TECs: TEC1, TEC2, and TEC3), thereby mitigating systematic errors [36]. By adopting the developed control method, the system would reach a stable state as soon as possible.

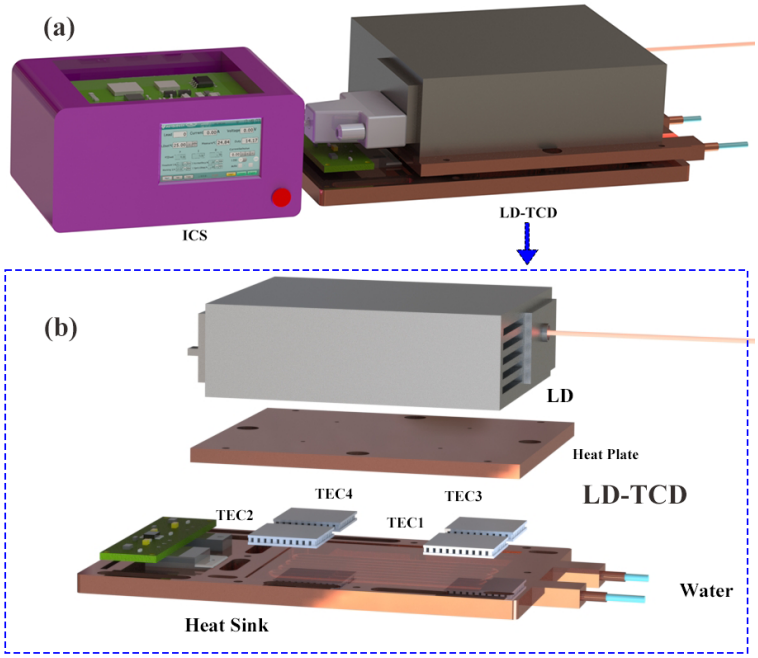

Figure 1. Device diagram of intelligent LD temperature controller. (**a**) Intelligent control system (ICS); (**b**) LD temperature control device (LD-TCD).

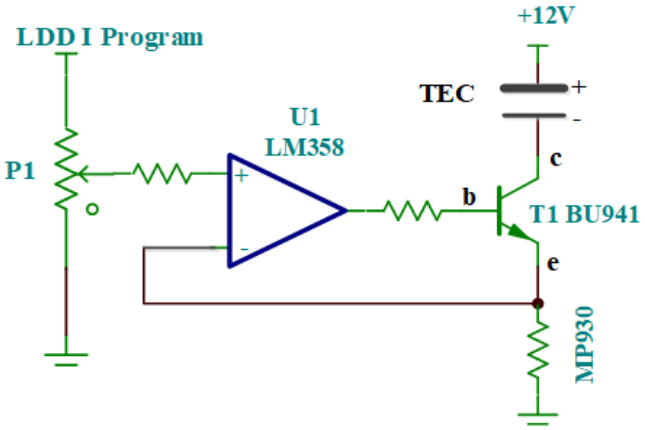

Figure 2. The constant-current-source circuit for fast temperature control unit. b, Base; c, Collector; e, Emitter.

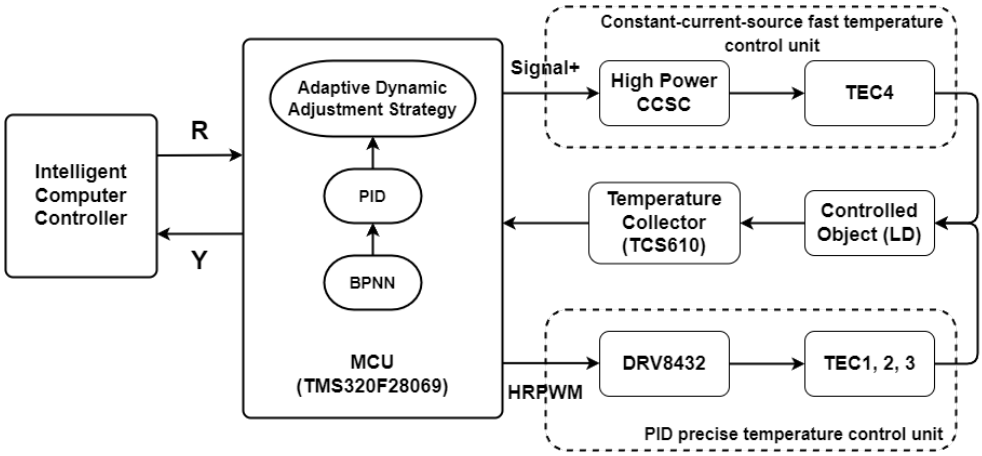

Figure 3. Framework of the control system. R is the desired output value, and Y is the actual output value. MCU, micro control unit; PID, proportional-integral-derivative algorithm; HRPWM, high-resolution pulse-width modulation; TEC, thermoelectric cooler; CCSC, constant-current-source circuit.

To improve the performance of the LD temperature controller, a BPNN-optimized PID controller with an ADAS was designed to dynamically adjust the PID parameters within the system. Due to the computational power and calculation speed limitation of the MCU, the system selected the classical and simple BPNN algorithm with one hidden layer in Figure 4. The structure of the BPNN-PID controller consisted of four input layer neurons, eight hidden layer neurons, and three output layer neurons. A random number generation method was employed to optimize and compare the initial weights of the BPNN after calculating the systematic error e from the input r and output y. To normalize the neurotransmitters and transform the input signal into the output signal, $tanh(j)$ and $sigmoid(k)$ were employed as activation functions [37]. Then, the BPNN dynamically adjusted the PID parameters kp, ki, kd to compute the optimal control output u. Finally, the output y was derived by applying u to the controlled object. In this process, the golden division method was adopted to determine the number of hidden layer neurons H_j [38]. The parameter values $i(1 \sim 4)$, $j(1 \sim 8)$, and $k(1 \sim 3)$ were used to denote the number of neurons in each layer. After the online learning of the BPNN [39], better PID control parameters were acquired.

The network between the input layer and the hidden layer was represented as $net_{1j} = \sum_{i=1}^{4} v_{ij} \cdot X_i$. Therefore, the procedure for calculating the values of the hidden layer neurons was expressed:

$$H_j = net_{1j} \cdot tanh(j) \tag{1}$$

After that, the network between the hidden layer and the output layer was represented as $net_{2k} = \sum_{j=1}^{8} \omega_{jk} \cdot H_j$. Thus, three neurons of the output layer were set:

$$\begin{cases} K_p = O_{k=1} = net_{2k} \cdot sigmoid(k) \\ K_i = O_{k=2} = net_{2k} \cdot sigmoid(k) \\ K_d = O_{k=3} = net_{2k} \cdot sigmoid(k) \end{cases} \tag{2}$$

Lastly, the control quantity, u, for the BPNN-PID controller was set:

$$u(n) = u(n-1) + K_p \cdot \Delta e(n) + K_i \cdot e(n) + K_d \cdot [\Delta e(n) - \Delta e(n-1)] \tag{3}$$

where the calculation of $u(n)$ was represented as the duty cycle of the HRPWM output from the MCU. Because the maximum duty cycle of HRPWM in our MCU was 200, the value of u could change from -200 to 200 according to the temperature difference.

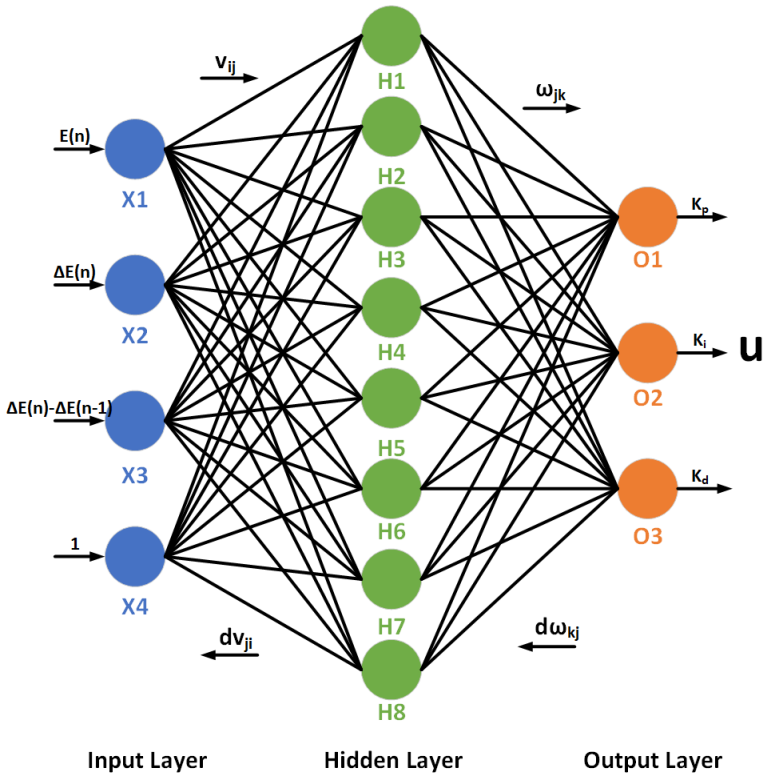

Figure 4. The structure of BPNN.

It is well known that the BPNN aimed to find the minimum value of the cost function ($E = \varphi \cdot (r - y)^2$, φ = 0.5, y, the actual outputs, r, the desired values) by adjusting the weights based on the real-time error signal and the gradient descent method. During the backpropagation process, the weights of the neural network were updated,

$$\Delta v(n) = -\eta \cdot \frac{\partial E(n)}{\partial v(n)} + \alpha \cdot \Delta v(n-1) \tag{4}$$

where η and α denoted the learning rate and the inertia coefficient, respectively. In our experiment, $\eta = 0.01$ and $\alpha = 0.1$. And the weights ($d\omega_{kj}$ and dv_{ji}) were calculated by employing the sigmoid function ($sign(n)$), the chain rule, and the incremental PID algorithm.

On this basis, an ADAS was proposed to make the PID precise temperature control unit cooperate organically with the fast temperature control unit. The heat generated by the LD exhibited a positive correlation with its operating current [40,41]. Given that the LD's operating current ranged from 0 to 65 A, and the system utilized a 16-bit DAC, the control quantity y_h was determined,

$$y_h = h \cdot \frac{H_s \cdot (2^{16} - 1)}{65} \tag{5}$$

where h and H_s are the scale factor and the set current of the LD, respectively.

The total control quantities Y_{output} of the system was expressed

$$\begin{cases} Y_{output} = \alpha \cdot y_h + \beta \cdot u \\ \alpha = \sigma \cdot \left(\frac{|e[n]|}{|T_s[n] - T_m[0]|} + \sigma_0\right) \\ \beta = \mu \cdot \left(\frac{||T_s[n] - T_m[0]| - |e[n]||}{|T_s[n] - T_m[0]|} + \mu_0\right) \end{cases} \tag{6}$$

where $T_s[n]$, $e[n]$, and $T_m[0]$ are the setting temperature, systematic error value, and initial temperature, respectively. $\alpha \cdot y_h$ and the $\beta \cdot u$ are the controlled quantity of the constant-current-source fast temperature control unit and the controlled quantity for the BPNN-PID temperature controller, respectively. σ and μ are used as conditional selection values to determine the activation or deactivation of two control units, which were consistently set to 1 in our experimental setup. Additionally, σ_0 and μ_0 were established as constants to regulate the control performance across different systems. As a result, the adaptive conditional values α, β were introduced to optimize the control amount of the above two units.

The BPNN-PID with ADAS is illustrated in Figure 5. Initially, the system started the temperature acquisition and calculated the system error. The BPNN algorithm was employed to optimize the PID parameters based on the real-time temperature difference, so that the control quantity was dynamically adjusted to make the LD temperature reach the set value as soon as possible. When the current was uploaded to the LD, significant heat was instantaneously generated, and a constant-current-source unit was employed to facilitate rapid cooling during the LD current injection process. Meanwhile, an adaptive dynamic adjustment strategy (ADAS) was developed to optimize the performances of the above two control units. In this case, when the error was the largest, α reached its maximum value, whereas β reached its minimum value. Then, α and β decreased and increased with the decrease in the error during system operation, respectively. In other words, when the temperature difference diminished, the influence of the first unit ($\alpha \cdot y_h$) gradually declined, while the influence of the second unit ($\beta \cdot u$) progressively increased.

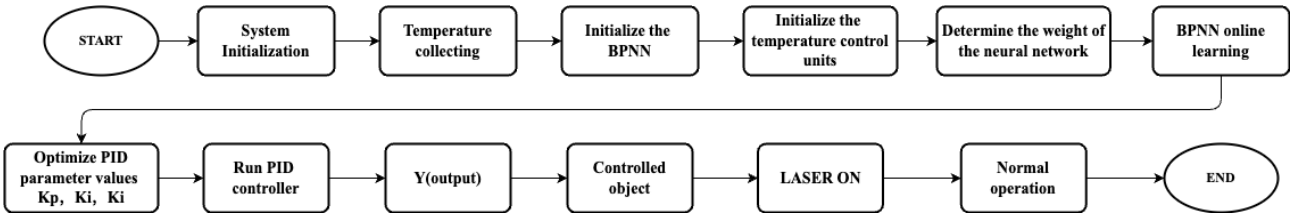

Figure 5. Flow chart of the BPNN-PID algorithm with the adaptive dynamic adjustment strategy (ADAS).

3. Experimental Results

To systematically evaluate and compare the performances of the three temperature controllers, including the conventional PID controller, the BPNN-PID controller, and the BPNN-PID with ADAS controller, we meticulously recorded the temperature variation of an LD and the step response. Firstly, the temperatures of the cooling water circulator and the LD were set as 18.00 °C and 24.97 °C, respectively, and the parameter values of the conventional PID controller were set as $Kp = 9, Ki = 1, Kd = 0.5$. Based on extensive empirical testing, the values for σ_0 and μ_0 in our system were set to 1.2 and 1.5 in Equation (6), respectively. After achieving the temperature stability control of LD in 510 s based on the above three temperature controllers, the power supply current of the LD was rapidly increased from 0 A to 51 A (operating voltage: 3.95 V), the output optical power of the LD and the generated heat power were 110.95 W and about 100 W, respectively. In this case, the temperature variation trend was recorded and shown in Figure 6. It was seen that for the conventional PID controller, the maximum temperature reached 27.94 °C, and the temperature achieved stability after 1300 s (Curve (a)). When the conventional PID controller was replaced by the BPNN-PID controller, the maximum temperatures and the time achieving a stable state decreased to 27.28 °C and 875 s (Curve (b)), respectively. Further, when they were replaced by the BPNN-PID with ADAS controller, the maximum

temperatures and the times achieving stable state decreased to 26.55 °C and 350 s (Curve (c)), respectively.

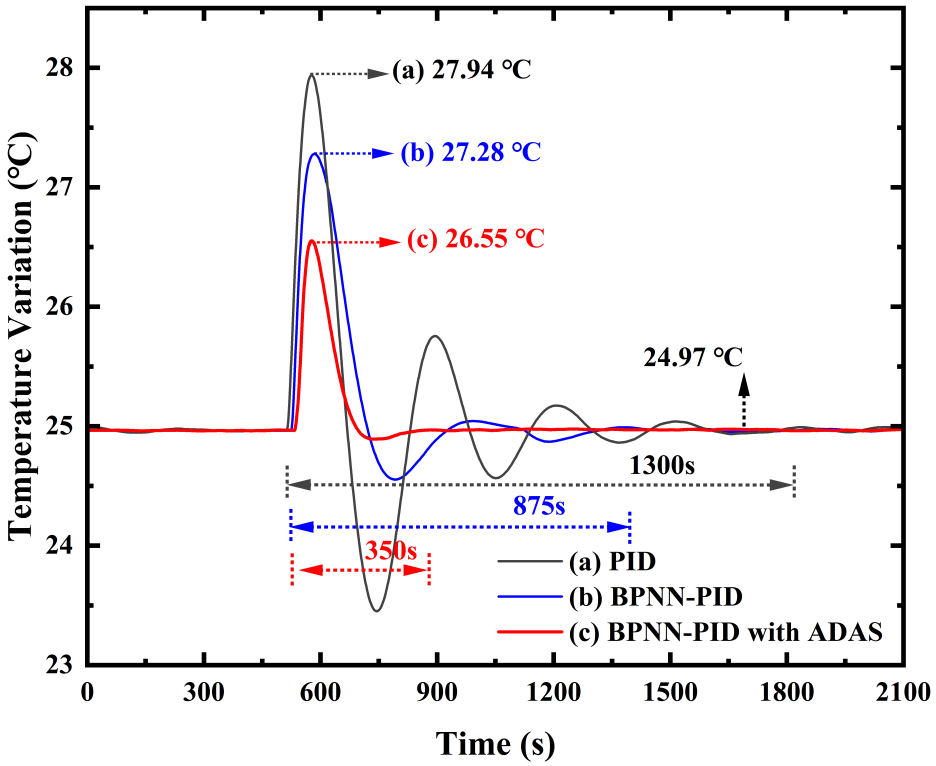

Figure 6. The temperature variation of LD with 100 W thermal power. (**a**) PID, 27.94 °C (Maximum), (**b**) BPNN-PID, 27.28 °C (Maximum), and (**c**) BPNN-PID with ADAS, 26.55 °C (Maximum).

On this basis, the long-term temperature stability of the LD over 7200 s was also measured and illustrated in Figure 7. It was obvious to see that the temperature stability (Curve (c)) for the BPNN-PID with ADAS controller was better than ±0.082%, which was better than ±0.146% for the BPNN-PID controller (Curve (b)) and ±0.148% for the conventional PID controller (Curve (a)).

At the same time, the step response was also investigated by increasing the set temperature of LD from 24.97 °C to 26.97 °C at a rate of 1 °C/s, and the results are depicted in Figure 8. It was clear that the overshoot and time achieving the steady state of the BPNN-PID with ADAS were 210 s and 1.105%, respectively, which was better than 540 s and 1.746% for BPNN-PID as well as 960 s and 3.181% for the conventional PID. In a word, the results revealed that the BPNN-PID with ADAS temperature controller could quickly stabilize the temperature of an LD with 100 W thermal power, and the system showed excellent control performance.

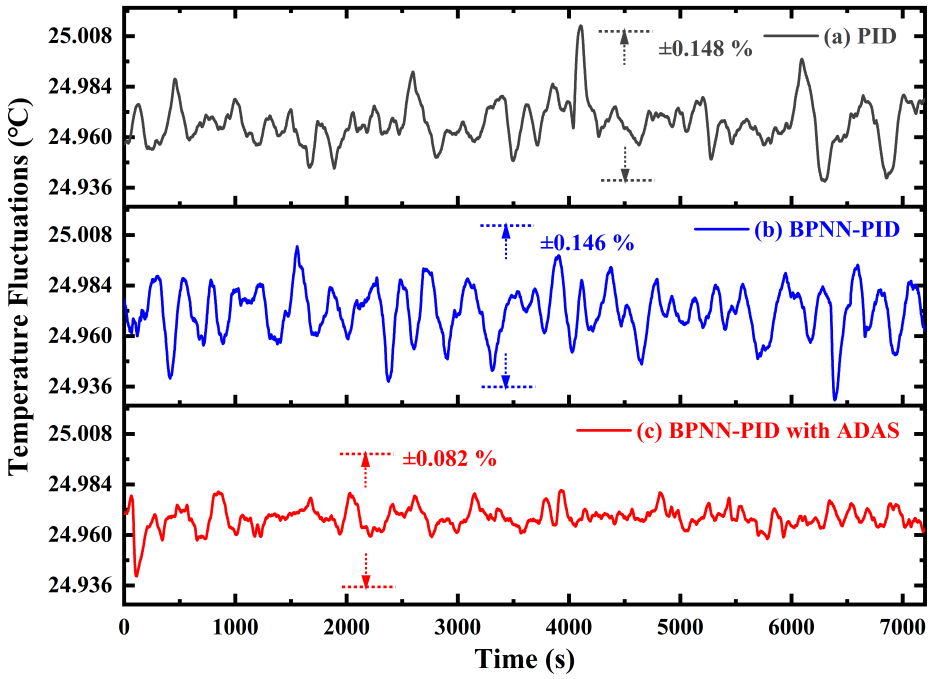

Figure 7. The temperature fluctuations of LD with 100 W thermal power using the three types of controller. (**a**) PID, (**b**) BPNN-PID, and (**c**) BPNN-PID with ADAS.

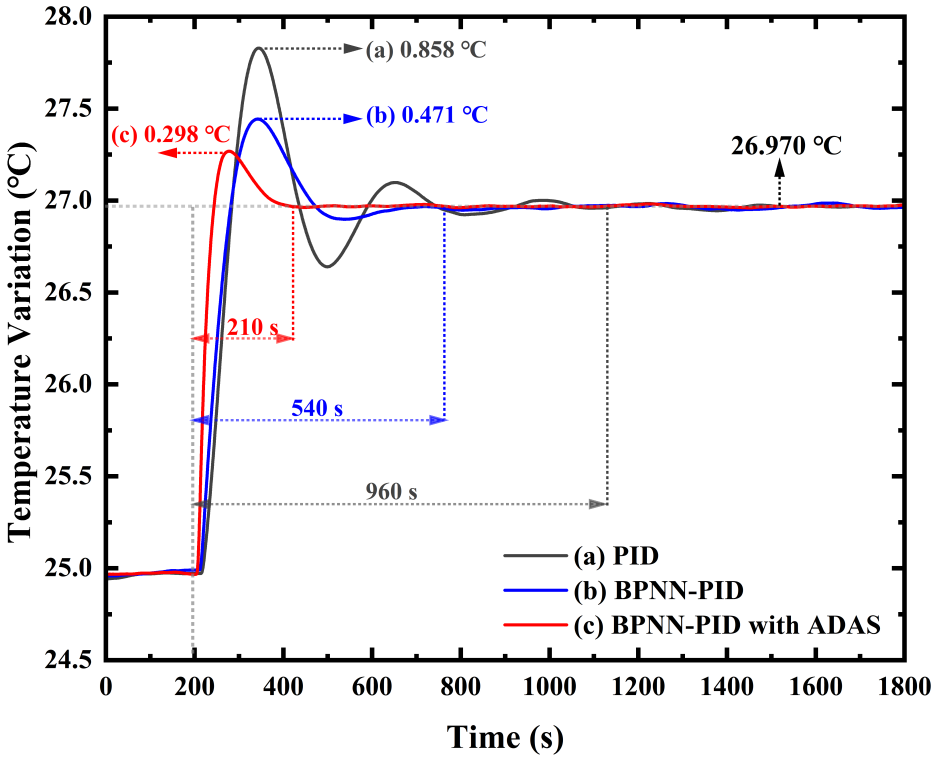

Figure 8. The step response of different controllers. (**a**) PID, 0.858 °C (Overshoot), (**b**) BPNN-PID, 0.471 °C (Overshoot), and (**c**) BPNN-PID with ADAS, 0.298 °C (Overshoot).

4. Discussions

In the experimental results, a temperature control system with a thermal power of 100 W LD was implemented. The extensive experimental testing results have shown that the presented method provided efficient and stable temperature control at room temperature for LDs used as pump sources in a variety of high-power lasers, including all-solid-state

lasers and fiber lasers. When a large current was loaded into the LD, the LD experienced an instantaneous thermal transient. For the conventional PID control algorithm, the constant parameters (P, I, D) led to its poor adaptability to this abrupt thermal load system. As shown in the experimental results, the serious temperature overshoot (2.97 °C) and long stability time (1300 s) were observed by using a conventional PID controller in Figure 6. Compared to the conventional PID controller, the BPNN-PID demonstrated improvements of 32.69% in stability time, 1.35% in temperature stability, and 43.75% in step response time. These good results benefited from the fact that the BPNN algorithm could perform online learning and adjust parameters in real time to cope with the dynamic environment. However, because it took time to train and online learn according to the temperature difference, the response was so relatively slow at the beginning that it was difficult to deal with this dynamic. As a result, the oscillation period of BPNN-PID was actually longer than the PID in Figure 6. In order to address this issue, a constant-current-source circuit was integrated into the BPNN-PID controller to reduce the computational burden of BPNN, which facilitated heat transfer from the top of the heat plate to the bottom of the heat sink. On this basis, an adaptive dynamic adjustment strategy (ADAS) was established to optimize and adjust the temperature control units to reach the set point as rapidly as possible and realize temperature stability over an extended period. The results demonstrated that the BPNN-PID with ADAS achieved a 73.1% and 60% improvement in stability time compared to the conventional PID controller and the BPNN-PID, respectively, and the oscillation period was the shortest, as shown in Figure 6. As shown in Figure 7, the temperature stability achieved using BPNN-PID with ADAS improved by 44.59% and 43.84% compared to the PID and BPNN-PID controllers, respectively. Meanwhile, the step response time results presented in Figure 8 demonstrated that the developed method enhanced the response speed by 78.1% and 61.1% relative to the other two methods. Moreover, it was expected to employ more advanced algorithms and MCU to further optimize the initial weights and parameter values of the BPNN-PID with ADAS, thereby enhancing its robustness and applicability.

5. Conclusions

In a word, a machine learning-based temperature controller for high-power LDs was demonstrated in this paper. By integrating a constant-current-source circuit into the conventional PID temperature-controlling circuit, the temperature-controlling speed can be effectively increased. On this basis, a BPNN with an adaptive dynamic adjustment strategy (ADAS) was established to actively optimize and adjust the temperature control unit by performing real-time analysis of temperature differentials, thereby enhancing its capability to efficiently manage significant temperature fluctuations caused by high heat and achieving rapid and stable temperature regulation. As a result, when the power supply current of the LD was rapidly increased from 0 A to 51 A (operating voltage: 3.95 V), the reached maximum temperature was only 26.55 °C, and the temperature achieved a steady-state in as little as 350 s. The long-term temperature fluctuation was lower than ±0.082%. Moreover, when the set value of the temperature was changed from 24.97 °C to 26.97 °C at a rate of 1 °C/s, the time in which the temperature achieved steady state was as short as 210 s. The presented results revealed the superiority of the machine learning-based BPNN-PID with ADAS temperature controller, and we believe that the presented method can pave the way to developing a novel temperature controller for an LD with higher output power. In order to further enhance the output performance of the laser, more sophisticated machine learning methods based on deep neural networks would be applied to the laser system. Meanwhile, advanced processing systems such as FPGA would be

employed to stably control the temperatures of key optical elements, precisely lock the cavity length, optimize the beam quality, and further suppress noise.

Author Contributions: Conceptualization, Y.H., X.J. and P.J.; software, Y.H., X.J. and P.J.; investigation, Y.H., X.J., P.J., J.S. and H.L.; writing—original draft preparation, Y.H. and F.L.; writing—review and editing, X.J., P.J. and H.L.; supervision, H.L.; project administration, H.L.; funding acquisition, H.L. All authors have read and agreed to the published version of the manuscript.

Funding: This work was supported by the National Key Research and Development Program of China (2022YFC2204003), the Research Project Supported by Shanxi Scholarship Council of China (No. 2022-015), the Special fund for Science and Technology Innovation Teams of Shanxi Province (202204051002005), the first Lab-National Innovation Center (Shanxi) science and technology innovation project, and the National Key Laboratory of Particle Transport and Separation Technology (KWKF-2024-2).

Institutional Review Board Statement: Not applicable.

Informed Consent Statement: Not applicable.

Data Availability Statement: Data are contained within the article.

Conflicts of Interest: The authors declare no conflicts of interest.

References

1. Sokolowski, W.; Hangst, A.; Buehler, M.; Killi, A.; Ryba, T.; Benz, S.; Armbruster, B.; Olschowsky, P. Latest developments in high brightness diode lasers and their applications. In Proceedings of the Photonics West—Lasers and Applications in Science and Engineering, San Francisco, CA, USA, 2–7 February 2013. [CrossRef]
2. Gao, S.; Gong, M.; Liu, H.; Wang, D. Influence of LD temperature fluctuation on the performance of corner-pumped TEM00 CW composite Nd:YAG laser. *Laser Phys.* **2010**, *20*, 790–792. [CrossRef]
3. Álvarez, J.; Pimienta, J.; Mercado, E.; Sarmiento, R. An extended laser cavity centered at 780 nm for high-resolution laser spectroscopy applications. *Laser Phys.* **2023**, *33*, 055005. [CrossRef]
4. Tritt, T.M. Thermoelectric Materials: Principles, Structure, Properties, and Applications. In *Encyclopedia of Materials: Science and Technology*, 2nd ed.; Elsevier: Amsterdam, The Netherlands, 2002. [CrossRef]
5. Zhao, D.; Tan, G. A review of thermoelectric cooling: Materials, modeling and applications. *Appl. Therm. Eng.* **2014**, *66*, 15–24. [CrossRef]
6. Barker, J.; Khan, M.; Solomos, T. Mechanism of the Pasteur effect. *Nature* **1964**, *201*, 1126–1127. [CrossRef]
7. Bärwolff, A.; Puchert, R.; Enders, P.; Menzel, U.; Ackermann, D. Analysis of thermal behaviour of high power semiconductor laser arrays by means of the finite element method (FEM). *J. Therm. Anal. Calorim.* **1995**, *45*, 417–436. [CrossRef]
8. Puchert, R.; Menzel, U.; Bärwolff, A.; Voβ, M.; Lier, C. Influence of heat source distributions in GaAs/GaAlAs quantum-well high-power laser arrays on temperature profile and thermal resistance. *J. Therm. Anal. Calorim.* **1997**, *48*, 1273–1282. [CrossRef]
9. Ebert, T.; Treusch, H.G.; Loosen, P.; Poprawe, R. Optimization of microchannel heatsinks for high-power diode lasers in copper technology. In *Proceedings of the Fabrication, Testing, Reliability, and Applications of Semiconductor Lasers III*; Linden, K.J., Fallahi, M., Linden, K.J., Wang, S.C., Eds.; International Society for Optics and Photonics, SPIE: Bellingham, WA, USA, 1998; Volume 3285, pp. 25–29. [CrossRef]
10. Wang, Y. PID Temperature Control. In *Conveyor Belt Furnace Thermal Processing*; Springer International Publishing: Cham, Switzerland, 2018; pp. 63–76. [CrossRef]
11. Fong-Chwee, T.; Sirisena, H. Self-tuning PID controllers for dead time processes. *IEEE Trans. Ind. Electron.* **1988**, *35*, 119–125. [CrossRef]
12. Besharati Rad, A.; Lo, W.L.; Tsang, K. Self-tuning PID controller using Newton-Raphson search method. *IEEE Trans. Ind. Electron.* **1997**, *44*, 717–725. [CrossRef]
13. Åström, K.; Hägglund, T.; Hang, C.; Ho, W. Automatic Tuning and Adaptation for PID Controllers—A Survey. *IFAC Proc. Vol.* **1992**, *25*, 371–376. [CrossRef]
14. Xing, X.F.; Li, H.Z. Modeling and Simulation the Semiconductor Lasers Diode Temperature Controlling. *Adv. Mater. Res.* **2011**, *338*, 706–708. [CrossRef]

15. Cong, M.; Xu, W.; Wang, Y. Design of Temperature Controller for Laser Diode Based on DSP and Fuzzy-PID Control. In Proceedings of the 2010 International Conference on Electrical and Control Engineering, Wuhan, China, 25–27 June 2010; pp. 786–789. [CrossRef]
16. Jian, Y.; Deng, H. A FPGA-based real-time particle swarm optimization for temperature control of semiconductor laser. In Proceedings of the International Conference on Optoelectronic Materials and Devices (ICOMD 2022), Chongqing, China, 16–18 December 2022; Huang, Q., Ed.; International Society for Optics and Photonics, SPIE: Bellingham, WA, USA, 2023; Volume 12600, p. 126001S. [CrossRef]
17. Chen, K.Y.; Tung, P.C.; Tsai, M.T.; Fan, Y.H. A self-tuning fuzzy PID-type controller design for unbalance compensation in an active magnetic bearing. *Expert Syst. Appl.* **2009**, *36*, 8560–8570. [CrossRef]
18. Zhang, J.; Zhuang, J.; Du, H.; Wang, S. Self-organizing genetic algorithm based tuning of PID controllers. *Inf. Sci.* **2009**, *179*, 1007–1018. [CrossRef]
19. Gaing, Z.L. A particle swarm optimization approach for optimum design of PID controller in AVR system. *IEEE Trans. Energy Convers.* **2004**, *19*, 384–391. [CrossRef]
20. Chan, Y.F.; Moallem, M.; Wang, W. Design and Implementation of Modular FPGA-Based PID Controllers. *IEEE Trans. Ind. Electron.* **2007**, *54*, 1898–1906. [CrossRef]
21. Wu, H.; Su, W.; Liu, Z. PID controllers: Design and tuning methods. In Proceedings of the 2014 9th IEEE Conference on Industrial Electronics and Applications, Hangzhou, China, 9–11 June 2014; pp. 808–813. [CrossRef]
22. Borase, R.P.; Maghade, D.; Sondkar, S.; Pawar, S. A review of PID control, tuning methods and applications. *Int. J. Dyn. Control* **2021**, *9*, 818–827. [CrossRef]
23. Rahman, M.A.; Saleh, T.; Jahan, M.P.; McGarry, C.; Chaudhari, A.; Huang, R.; Tauhiduzzaman, M.; Ahmed, A.; Mahmud, A.A.; Bhuiyan, M.S.; et al. Review of Intelligence for Additive and Subtractive Manufacturing: Current Status and Future Prospects. *Micromachines* **2023**, *14*, 508. [CrossRef]
24. Zhou, Y.; Yang, Y.; Li, J.; Wang, F. PID Control in the Reactor Temperature Control System Based on BP Neural Network. In Proceedings of the 2009 International Conference on Intelligent Human-Machine Systems and Cybernetics, Hangzhou, China, 26–27 August 2009; Volume 1, pp. 245–248. [CrossRef]
25. Aliqab, K.; Sohaib, M.A.; Ali, F.; Armghan, A.; Alsharari, M. Employment of Self-Adaptive Bayesian Neural Network for Systematic Antenna Design: Improving Wireless Networks Functionalities. *Micromachines* **2023**, *14*, 594. [CrossRef]
26. Qiao, H.; Peng, W.; Jin, P.; Su, J.; Lu, H. Performance Improvement of Single-Frequency CW Laser Using a Temperature Controller Based on Machine Learning. *Micromachines* **2022**, *13*, 1047. [CrossRef] [PubMed]
27. Li, C.H.; Xu, S.X.; Xie, Y.; Zhao, J. The Application of PSO-BP Neural Network PID Controller in Variable Frequency Speed Regulation System. *Appl. Mech. Mater.* **2014**, *599*, 1090–1093. [CrossRef]
28. Shi, Y.; Eberhart, R.C. Parameter Selection in Particle Swarm Optimization. In *Evolutionary Programming VII, Proceedings of the 7th International Conference, EP98, San Diego, CA, USA, 25–27 March 1998*; Springer: Berlin/Heidelberg, Germany, 1998. [CrossRef]
29. Wang, Y.; Liu, J.; Li, R.; Suo, X.; Lu, E. Application of PSO-BPNN-PID Controller in Nutrient Solution EC Precise Control System: Applied Research. *Sensors* **2022**, *22*, 5515. [CrossRef]
30. Åström, K.; Hägglund, T. The Future of PID Control. *IFAC Proc. Vol.* **2000**, *33*, 19–30. [CrossRef]
31. Liu, X.; Zhao, W.; Xiong, L.; Liu, H. Thermal Design and Management in High Power Semiconductor Laser Packaging. In *Packaging of High Power Semiconductor Lasers*; Springer: New York, NY, USA, 2015; pp. 53–88. [CrossRef]
32. Yang, S.; Zhang, J.Y.; Yang, Y.Y.; Huang, J.Y.; Bai, Y.R.; Zhang, Y.; Lin, X.C. Automatic compensation of thermal drift of laser beam through thermal balancing based on different linear expansions of metals. *Results Phys.* **2019**, *13*, 102201. [CrossRef]
33. Peng, W.; Jin, P.; Li, F.; Su, J.; Lu, H.; Peng, K. A Review of the High-Power All-Solid-State Single-Frequency Continuous-Wave Laser. *Micromachines* **2021**, *12*, 1426. [CrossRef] [PubMed]
34. Yin, Q.; Lu, H.; Su, J.; Peng, K. High power single-frequency and frequency-doubled laser with active compensation for the thermal lens effect of terbium gallium garnet crystal. *Opt. Lett.* **2016**, *41*, 2033–2036. [CrossRef]
35. Chen, M.; Li, I.; Hu, C. The Driver Circuit and Focusing Lens Designed for the Laser Range-Finder. *Key Eng. Mater.* **2008**, *364–366*, 160–165. [CrossRef]
36. Jin, X. Study on A High-Precision Digital Temperature-Control System for All-Solid-State Single-Frequency Green Laser. *Chin. J. Lasers* **2015**, *42*, 0902010. [CrossRef]
37. Rumelhart, D.E.; Hinton, G.E.; Williams, R.J. Learning representations by back-propagating errors. *Nature* **1986**, *323*, 533–536. [CrossRef]
38. Jiang, Q.; Huang, R.; Huang, Y.; Chen, S.; He, Y.; Lan, L.; Liu, C. Application of BP Neural Network Based on Genetic Algorithm Optimization in Evaluation of Power Grid Investment Risk. *IEEE Access* **2019**, *7*, 154827–154835. [CrossRef]
39. Allaf, N.A. Improving the Performance of Backpropagation Neural Network Algorithm for Image Compression/Decompression System. *J. Comput. Sci.* **2010**, *6*, 1347–1354. [CrossRef]

40. Lan, Y.; Yang, G.; Liu, Y.; Zhao, Y.; Wang, Z.; Li, T.; Demir, A. 808 nm broad-area laser diodes designed for high efficiency at high-temperature operation. *Semicond. Sci. Technol.* **2021**, *36*, 105012. [CrossRef]
41. Bowman, S.R. High-power diode-pumped solid-state lasers. *Opt. Eng.* **2012**, *52*, 021012. [CrossRef]

Disclaimer/Publisher's Note: The statements, opinions and data contained in all publications are solely those of the individual author(s) and contributor(s) and not of MDPI and/or the editor(s). MDPI and/or the editor(s) disclaim responsibility for any injury to people or property resulting from any ideas, methods, instructions or products referred to in the content.